Bioelectromagnetics 43:355–367 (2022)

Vestibular Extremely Low-Frequency Magnetic and Electric Stimulation Effects on Human Subjective Visual Vertical Perception

Nicolas Bouisset[1,2] **Sébastien Villard**[1,2] **and Alexandre Legros**[1,2,3,4,5,6]*

[1]*Human Threshold Research and Bioelectromagnetics Group, Imaging, Lawson Health Research Institute, London, Canada*
[2]*Department of Kinesiology, Western University, London, Canada*
[3]*Department of Medical Biophysics, Western University, London, Canada*
[4]*Department of Medical Imaging, Western University, London, Canada*
[5]*Euromov Digital Heath in Motion, Univ Montpellier, IMT Mines Ales, Montpellier, France*
[6]*EuroStim, Montpellier, France*

Electric fields from both extremely low-frequency magnetic fields (ELF-MF) and alternating current (AC) stimulations impact human neurophysiology. As the retinal photoreceptors, vestibular hair cells are graded potential cells and are sensitive to electric fields. Electrophosphene and magnetophosphene literature suggests different impacts of AC and ELF-MF on the vestibular hair cells. Furthermore, while AC modulates the vestibular system more globally, lateral ELF-MF stimulations could be more utricular specific. Therefore, to further address the impact of ELF-MF-induced electric fields on the human vestibular system and the potential differences with AC stimulations, we investigated the effects of both stimulation modalities on the perception of verticality using a subjective visual vertical (SVV) paradigm. For similar levels of SVV precision, the ELF-MF condition required more time to adjust SVV, and SVV variability was higher with ELF-MF than with AC vestibular-specific stimulations. Yet, the differences between AC and ELF-MF stimulations were small. Overall, this study highlights small differences between AC and ELF-MF vestibular stimulations, underlines a potential utricular contribution, and has implications for international exposure guidelines and standards. Bioelectromagnetics. 43:355–367, 2022 © 2022 Bioelectromagnetics Society.

Keywords: **extremely low-frequency magnetic fields; magnetic induction; alternating current stimulation; human vestibular system; subjective visual vertical**

INTRODUCTION

Electric fields (E-Fields) applied to the human vestibular systems modulate their hair cell activity [Zenner et al., 1992; Norris et al., 1998; Gensberger et al., 2016; Dlugaiczyk et al., 2019].

The most well-known and reported means for such vestibular-specific E-Fields modulation involves applying direct (DC) or alternating (AC) electric currents to the mastoid processes (for review, see Fitzpatrick and Day [2004]).

Since Michael Faraday's work, we know that variations in magnetic flux density over time (dB/dt measured in T/s) also generate E-Fields and currents in conductors, such as the human body, via magnetic

Nicolas Bouisset and Sébastien Villard contributed equally to this study.

Conflicts of interest: None.

*Correspondence to: Alexandre Legros, Imaging Department, Lawson Health Research Institute, and Departement of Medical Biophysics, Western University, 268 Grosvenor St., London, ON, N6A 4V2, Canada.
E-mail: alegros@uwo.ca

Received for review 13 May 2021; Revised 25 May 2022; Accepted 18 June 2022

DOI:10.1002/bem.22417
Published online 08 July 2022 in Wiley Online Library (wileyonlinelibrary.com).

induction. Interestingly, some evidence shows that induced E-Fields from time-varying magnetic fields (MF) can modulate the vestibular system activity [Laakso et al., 2013; Van Nierop et al., 2013; Schaap et al., 2015].

Vestibular hair cells are found in the semicircular canals as well as in the otoliths (composed of the saccules and the utricles), respectively sensing small linear and angular head accelerations. Their high responsiveness resides in the fact that they are graded potential cells [Juusola et al., 1996a]. Compellingly, graded potential cells are also found within the retinal photoreceptors which, as the vestibular hair cells, are also easily triggered by small E-Fields [Attwell, 2003]. Indeed, the retinal graded potential cells detect small in situ E-Field variations and transduce this information into a visual phenomenon called phosphenes [Attwell, 2003]. Phosphenes are defined as the perception of flickering lights in the peripheral visual field. They can be produced by both AC (Electrophosphenes) and time-varying MF (Magnetophosphenes) [Lövsund et al., 1979].

To date, international recommendations and standards regarding the general public and workers' exposure to the so-called extremely low-frequency magnetic fields (ELF-MF; <300 Hz) are based on magnetophosphene perception [IEEE, 2002; ICNIRP, 2010], as it is the most reliable systematic neurophysiological response documented to date. Yet, given the vestibular hair cells' high sensitivity to very small currents, they could represent another likely target of the ELF-MF-induced E-Fields. If so, this could also be critical from a public health perspective.

Previous work from our group [Bouisset et al., 2020a,b] suggested that both application and orientation of ELF-MF might preferentially target the vestibular otolithic subsystems. Particularly, a monaural lateral ELF-MF stimulation at the mastoid level would preferentially expose the utricle [Bouisset et al., 2020a]. Although the physiological frequency range for the vestibular hair cells peaks at 30 Hz during strenuous efforts [Carriot et al., 2014], these cells can still pick up information with frequencies above 2000 Hz [Curthoys, 2017]. Furthermore, the weighting of otolithic input is more likely to increase as stimulation frequencies rise [Carriot et al., 2015]. Therefore, at powerline frequencies (50/60 Hz), otolithic information is more likely to be much more predominantly integrated than canalithic inputs. Moreover, a specific utricle assessment, known as ocular vestibular-evoked myogenic potentials (oVEMPS) [Curthoys, 2010; Curthoys et al., 2018], shows that when subjected to head vibrations, utricles are best tuned at 100 Hz as eye muscle responses progressively decrease above and under this frequency [Todd et al., 2008, 2009; Zhang et al., 2012]. Remarkably, head vibration perception emerges when the vestibular systems are stimulated by AC currents above 5 Hz [Stephan et al., 2005]. However, above such frequency the vestibular system integrates an AC signal as a head vibration. Furthermore, when electrical vestibular stimulations are applied, the frequency response of vestibular reflexes are similar to the response obtained with mechanical stimuli [Fitzpatrick et al., 1996; Pavlik et al., 1999; Dakin et al., 2007; Forbes et al., 2013]. Interestingly, oVEMPS are still high at 50 Hz [Todd et al., 2008], indicating that E-Fields at powerline frequency could modulate otolithic function.

As shown in orbital flight research, the otoliths sense the linear-pull of gravity and, therefore, greatly contribute to the assessment of verticality [Oman, 2007]. One of the most used spatial orientation tasks is the subjective visual vertical (SVV). The SVV is the measure of the angle between the perceived vertical and the "true" (gravitational) vertical [Akin and Murnane, 2009]. The SVV is multimodal, relying on visual, proprioceptive, and cortical afferences, but it is known as primarily linked to the vestibular function [Friedmann, 1970; Dalmaijer, 2018]. In fact, the capability of perceiving verticality has been more specifically related to the vestibular otolithic function [Kumagami et al., 2009] and utricular activation, in particular, when the head is held upright [Jaeger et al., 2008].

The SVV is very sensitive to a variety of vestibular stimulations including DC [Zinc et al., 1997; Zink et al., 1998; Mars et al., 2001; Volkening et al., 2014]. The literature showing SVV modulations with transcranial electric stimulation applied at the mastoid processes is particularly interesting when studying ELF-MF upon the vestibular system because it suggests that induced E-Fields targeting the vestibular organs might indeed generate changes on a vestibular task.

For DC, the effect is well-documented as a misperception of SVV towards the anodal electrode [Zinc et al., 1997; Zink et al., 1998; Mars et al., 2001; Volkening et al., 2014]. A metanalysis of Zink and colleagues [1998] presented the relationship between SVV and ocular rotation [Dalmaijer, 2018]. It showed that while SVV misperception increases linearly with the stimulation current, the ocular torsion, on the other hand, increases following a negative exponential curve [Dalmaijer, 2018]. From the model provided in Dalmaijer's work, we can assess that with a 2 mA DC stimulation, about 70% of SVV measurement can be interpreted as originating from ocular torsion. It is therefore likely that an alternating ocular rotation, due to the changing polarity of the time-varying E-Fields, would modulate SVV results.

Electrophosphenes and magnetophosphene differences have been acknowledged for decades [Lövsund et al., 1980b]. Indeed, the head's anatomical structures such as bone, cerebrospinal fluid, and skin could dampen the E-Fields generated by AC [Srinivasan et al., 1998; Laakso and Hirata, 2013]. However, such a mechanism is not expected with ELF-MF given that they penetrate all structures without impediment. For the same reasons, the vestibular hair cells could be impacted differently whether they are stimulated with electric currents through the skull or with the non-hindered ELF-MF. Furthermore, electrical vestibular stimulations globally impact the entire system [Fitzpatrick and Day, 2004; Day et al., 2011; Kwan et al., 2019], whereas a monaural lateral ELF-MF could be more utricular specific [Bouisset et al., 2020a]. Therefore, given the similar neurophysiological properties between the hair cells and the photoreptors with regard to phosphene, we hypothesize that the SVV perception outcomes differ between AC and MF stimulations. We suggest that compared to the former, lateral monaural ELF-MF stimulations will more specifically affect the utricular system. Thus, we focused on the perception of verticality as a biomarker of the utricular performance and we compared the effects of both AC and ELF-MF vestibular stimulations, expecting to find greater modulation of verticality perception with the latter.

Methods

Participants

Thirty-three healthy participants (10 males, 24.6$\pm$4 years) took part in the experiment. We excluded participants with any self-reported history of vestibular-related pathology, chronic illnesses, neurological diseases affecting normal body movements, and prone to seizures. We also ruled out people self-reporting permanent metal devices above the neck or using recreational drugs. Moreover, because the SVV is a vestibular-specific test largely used to assess utricular function [Dieterich and Brandt, 1993, 2019; Böhmer and Rickenmann, 1995; Vibert et al., 1999; Min et al., 2007], all participants with SVV angle superior to $\pm$2.5° were also excluded from the final analysis. Such a process was done to make sure we did not bias the final results. Indeed, healthy participants can align the perceived vertical within $\pm$2° of the true gravitational vertical [Volkening et al., 2014]. Finally, we asked our participants to abstain from alcohol, nicotine, and caffeine intake for 24 h before the experiment to avoid any bias in the results [Antal et al., 2017]. This protocol was approved by Western University's Ethics Board for Health Science Research Involving Human Subjects (protocol #109161).

Stimulations. ELF-MF exposure was conveyed using a single-coil centered at the level of the left mastoid process (Fig. 1). We delivered ELF-MF exposures via a custom exposure system consisting of a 176-turn coil (11 turns of 16 layers over a length of 6.2 cm, 6 cm inner diameter, and 22 cm outer diameter) made of 5 mm wide hollow square copper wire. To dissipate the heat generated by the strong current flowing through the coils, a water-cooling system was integrated to the coil. Approximately 1800 W of excess heat was removed by letting cold ($\approx$ _10 °C) tap water circulate through the hollow copper tubing at a 0.8 L/min flow rate. Also, to favor participants' blinding to the different conditions, we minimized coil vibrations and sound production during the exposures

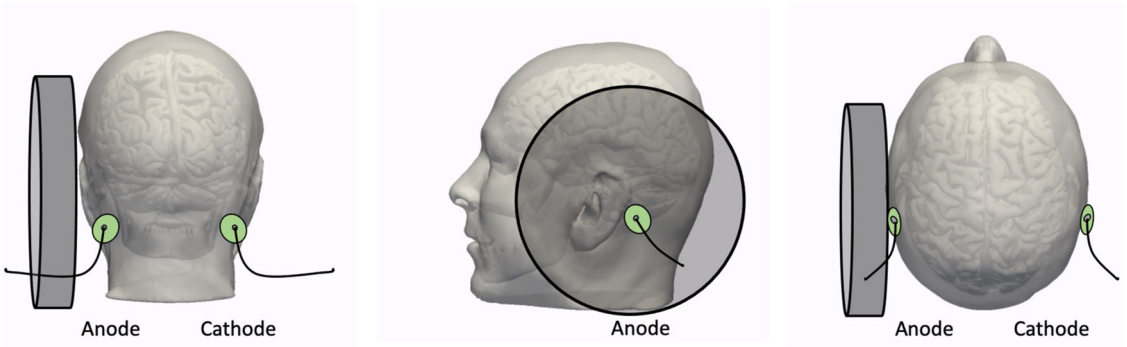

Fig. 1. Experimental stimulations. All three panels show both the MF custom coil system centered over the mastoid process and the binaural electrode montage (green circles) delivering the DC and AC currents. The left panel shows a view from behind, the middle panel shows a view from the left side, and the right panel a view from above. AC = alternating current; DC = direct current; MF = magnetic fields.

by impregnating the copper tubing with thermal epoxy as it was wound (i.e. wet winding technique). The coil was powered by an MTS magnetic resonance imaging (MRI) gradient amplifier array capable of delivering up to 200 A_{rms} at ±345 V (MTS Automation, Horsham, PA). The amplifier was driven by a command from a customized LabVIEW (2014 version 14.0.1 (32 bit), National Instrument, Austin, TX) script and a 16-bit National Instruments A/D Card (National Instrument).

We produced DC and AC with a transcranial current stimulation device (StarStim; Neuroelectrics, Barcelona, Spain), and the NIC software (Neuroelectrics Instrument Controller, version 1.4.1 Rev.2014-12-01, Barcelona, Spain) was used to drive the StarStim device via Bluetooth. In both electrical stimulations, a binaural bipolar montage (Anode-Left, Cathode-Right for DC) delivered electric stimulations at the mastoid processes (Fig. 1). The DC stimulation was used as a positive control condition. A positive control is defined herein as a condition in which specific known effects are expected [Johnson and Besselsen, 2002]. Indeed, based on the scientific literature, DC is known to, on average, bias SVV towards the anodal side of the stimulation [Mars et al., 2005; Volkening et al., 2014].

Following a double-blind within-subject repeated measure plan (Fig. 2), participants were exposed to (i) control trials (CTRL) with no stimulation, (ii) DC at 2 mA used as a positive control, (iii) AC stimulations (sinusoidal, peak ±2 mA) given at four frequencies (20, 60, 120, and 160 Hz), and (iv) alternating sinusoidal ELF-MF stimulations at the same frequencies.

As described by the following equation derived from Maxwell's third law:

$$E = \frac{r}{2}\frac{dB}{dt} = \pi r f B,$$

E represents the induced E-Fields, r the radius of the Faraday's loop encompassing a homogeneous alternating MF of flux density B, and frequency f. Thus, the intensity of the stimulation is linearly proportional to the frequency of stimulation. To compare similar intensity AC stimulations to ELF-MF stimulations, we decreased the flux density proportionally to the stimulation frequency to keep a constant dB/dt level (chosen to be 12.3 T s^{-1}) across frequencies. Table 1 summarizes the intensity levels reached at 3 cm from the casing of the coil where the vestibular system should be located [Yu et al., 2015].

For both ELF-MF and AC stimulations, we chose the frequencies following the subsequent rationale. As stated in the introduction, otoliths are best-tuned at 100 Hz, and responses progressively decline under and above this value [Todd et al., 2008, 2009; Zhang et al., 2012]. Therefore, we opted to investigate two frequencies above and two frequencies below 100 Hz. The main goal of this study is to study responses at 60 Hz (i.e. the powerline frequency in North America). Also, we chose 20Hz since AC stimulations up to such frequency generate ocular torsions [Mackenzie and Reynolds, 2018]. Finally, we kept both 120 and 160 Hz since otolithic responses drop dramatically at 200 Hz [Todd et al., 2008].

Procedure. This experiment consisted of a single session lasting about 1.5 h. After giving written informed consent, we equipped the participants with the electric stimulation device. We saturated the circular 25 cm^2 Ag/AgCl electrodes (StarStim,

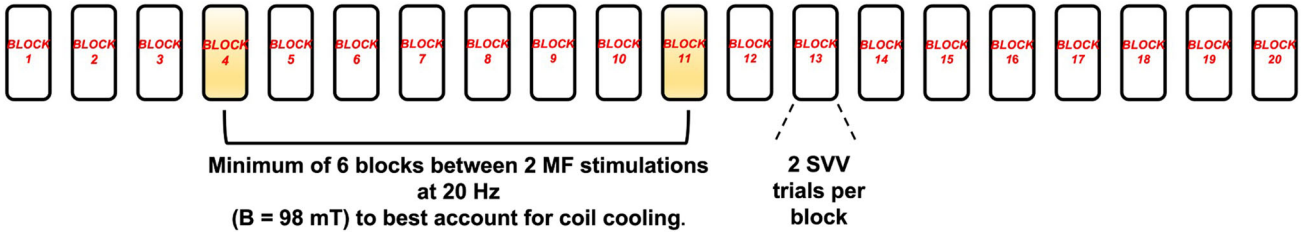

Fig. 2. Schematic representation of the protocol for one participant. Each session is made of 20 blocks. Each 30-s block represents one experimental condition: CTRL, DC, AC, or MF. Each AC and MF experimental condition was given at four different frequencies: 20, 60, 120, and 160 Hz. During each 30-s block, two consecutive SVV trials were executed. Block order is semi-randomized, as a minimum of six randomized blocks are set between two MF blocks at 20 Hz. A 1-min rest period is given between each experimental block. AC = alternating current; CTRL = control trials; DC = direct current; MF = magnetic fields.

TABLE. 1. Alternating Magnetic Field Intensity (in rms) Expressed in mT and T.s^{-1} at 3 cm from the Casing of the Coil for the Four Frequency Conditions

Intensity	20 Hz	60 Hz	120 Hz	160 Hz
***dB/dt* (T.s^{-1})**	12.3	12.3	12.3	12.3
Flux density B (mT)	98.0	32.8	16.4	12.3

Note: We intentionally decreased the level of flux density to keep a stable *dB/dt* across frequency conditions.

Neuroelectrics, Spain) with 8 ml of saline solution to provide proper conduction between the electrodes and the skin. We then secured the electrodes using the StarStim exposure cap and tape. To ensure appropriate stimulations, we maintained electrode impedances strictly below 10 kΩ throughout the experiment following the manufacturer's recommendations. Before starting the testing, we exposed the participants to 5-s DC (2 mA) and AC (peak ±2mA at 20 Hz) exposures while standing feet together, arms by their side, and eyes closed. This was done (i) to make sure that DC made participants sway towards the anodal side (for review see [Fitzpatrick and Day, 2004] and to ensure that the electrical stimulations were effective and (ii) as familiarization samples.

We asked the participants to sit on a sturdy stool, with their head upright, during the time of the experiment that occurred during a single session. To avoid any head movements adding noise to the results, we controlled for head position by constraining it against the coil support during all experimental trials. To avoid any environmental visual bias, we asked the participants to look through an open cone to a monitor displaying a dotted white line over a black background. The line was always oriented towards the left with a random starting angle bounded between −25 and −20°. All starting SVV angles were randomized between both trials and conditions throughout the experiment. Participants' eyes were 43 cm away from the screen displaying a 15-cm long dotted line, representing a visual angle of 23°. We asked the participants to use the wheel of a mouse to control the angle of this white line and align it with what they perceived to be the gravitational vertical. We instructed the participants to press the left button of the mouse to validate the measurement and record the final angle of the line when they reached the final alignment. They performed two consecutive measurements during one 30-s stimulation and repeated each stimulation twice for a total of 20 stimulations (Fig. 2). One-min rest periods were given between trials to avoid participant fatigue, dissipate the stimulation effects in between blocks, and prevent any carryover effects [Bresciani et al., 2002] (Fig. 2). A second investigator, blinded to the type of stimulation, was present at all times to position the participants correctly at the beginning of each trial and to make sure they maintained the proper positioning throughout the trials. To conceal the remaining faint noise generated by the coil, subjects wore earplugs throughout the experiment. We presented all conditions in a pseudo-randomized order, where higher flux density conditions (i.e. 20Hz) were distributed with a minimum of six trials from each other to allow for the proper cooling time of the coil (Fig. 2). We fully randomized all other stimulations.

Data collection and analysis. We collected the final angle of the line after adjustment (SVV), the initial angle of the line before the adjustment, and the adjustment time from the moment the line appeared on the screen to the button-click marking the final adjustment with a custom HTML/javascript program.

To account for the interindividual variability of SVV measurements and the known bias of the initial left angle of presentation [Pagarkar et al., 2013], we averaged the four measurements for each condition and subtracted the averaged SVV of each experimental condition from the CTRL averaged SVV. Thus, we obtained a difference to the CTRL value of the SVV angle that we will describe in the rest of this work as dSVVmean. We calculated the same difference for the standard deviations of the SVV over the four repetitions (dSVVstd). This dSVVstd represents how variable an adjustment was compared to the CTRL condition.

Finally, the vestibular system is implicated in spatial cognitive processes [Hitier et al., 2014]. Thus, time adjustment modulations could reflect potential cortical variations. Therefore, knowing that the initial angle was randomly generated between −25 and −20°, to compare the adjustment time for every condition and every participant, we computed an adjustment velocity as the angular distance between the initial angle and the final angle over the adjustment time. This variable was also averaged and presented as a difference to CTRL and called dVel.

The data analysis was performed with python (v.3.7.6; Python Software Foundation, Beaverton, OR) and R (v.3.6.0; Free Software Foundation, Boston, MA). A level of significance of $\alpha = 0.05$ was adopted throughout data analysis. dSVV variables were computed by subtracting the averaged SVV from the CTRL averaged SVV. Therefore, the dSVV for CTRL is equal to zero (dSVV CTRL = CTRL minus

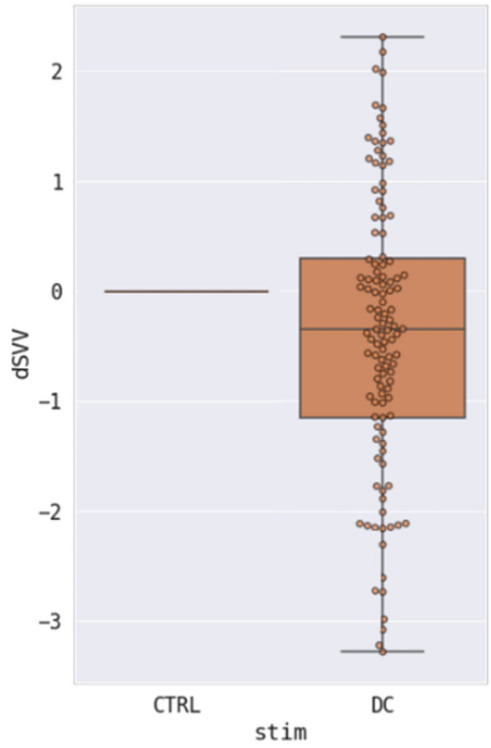

Fig. 3. Boxplot representation of dSVVmean between CTRL (left) and DC (right). dSVV CTRL is equal to CTRL minus CTRL (i.e. =0). DC is significantly lower than 0 (t29 = –2.0104, $P = 0.027$, $R^2 = 12\%$), which shows a mean misperception towards the anodal stimulation. AC = alternating current; CTRL = control trials; DC = direct current.

CTRL) (Fig. 3). Since the theoretical true vertical would correspond to a normal Gaussian distribution centered on zero, we implemented this distribution to the TRUE vertical condition. As a consequence, the effect of DC stimulations can be tested as DC versus CTRL (TRUE) (Fig. 3). Because averaged vestibular outcomes are always found biased toward the anodal side, a one-tailed one-sample *t*-test was conducted, with the expectation that dSVVmean for the DC condition would be below 0 (mean bias towards the anode expected).

We compared two stimulation types (AC and MF) and 4 stimulation frequencies (20, 60, 120, and 160 Hz) with two-way repeated measure analysis of variances (ANOVAs) on dSVVmean, dSVVstd, and dVel. We presented the generalized eta squared (η^2_G) as a measure of the effect size as it is recommended for repeated measure ANOVAs [Bakeman, 2005].

Results

The analysis of SVV angles showed that three participants demonstrated SVV angle >2.5° in the CTRL conditions. This suggests that these three participants could have undiagnosed vestibular dysfunctions. Thus, to avoid any result bias, we decided to classify these three participants as outliers and to remove them from the statistical analysis.

For positive control purposes, the results first consisted of comparing the effect of the DC stimulation on the perception of verticality (Fig. 3). By comparing the dSVV in the DC versus CTRL (TRUE) conditions, we tested if the DC condition was significantly lower than a condition with no stimulation. As expected [Mars et al., 2001; Volkening et al., 2014], the *t*-test showed that dSVV for the DC condition was on average significantly lower than 0 (t29 = −2.0104, $P = 0.027$, $R^2 = 12\%$), which describes a mean misperception towards the anodal stimulation on the left side (Fig. 3). The mean dSVV for DC was $-0.32 \pm 0.8°$.

Figure 4 presents the $dSVV_{mean}$, $dSVV_{std}$, and dVel results for both AC and MF stimulations. Two-way ANOVAs (two stimulation modalities × four frequencies) for repeated measures indicated no significant main effects of frequency conditions for $dSVV_{mean}$ ($F_{3,87} = 1.97$, $P = 0.12$), $dSVV_{std}$ ($F_{3,87} = 0.31$, $P = 0.82$), and dVel ($F_{3,87} = 1.70$, $P = 0.18$).

Similarly, no significant stimulation main effect was found for $dSVV_{mean}$ ($F_{1,29} = 0.6$, $P = 0.45$). However, $dSVV_{std}$ ($F_{1,29} = 7.86$, $P = 0.009$, $\eta^2_G = 2\%$) showed that while the variability of SVV is lower than CTRL for AC exposure, it is however greater than CTRL in the instance of MF stimulation (Fig. 4). Similarly, dVel ($F_{1,29} = 9.04$, $P = 0.005$, $\eta^2_G = 2\%$) showed that velocities to adjust the SVV measurement were greater in AC conditions than in the MF conditions (Fig. 4). Finally, no interaction effects were found for $dSVV_{mean}$ ($F_{3,87} = 1.87$, $P = 0.14$), $dSVV_{std}$: ($F_{3,87} = 0.76$, $P = 0.52$), or for dVel: ($F_{3,87} = 0.27$, $P = 0.84$).

Discussion

The current international standards and guidelines consider the impact of ELF-MF on neural networks through the paradigm of phosphene perception [ICNIRP, 2010; IEEE, 2019]. The current hypothesis regarding phosphenes is that they result from membrane potential modulations of graded potential retinal cells, impacting in cascade the continuous release of neurotransmitters through their ribbon synapses [Attwell, 2003]. Yet, the International Commission on Non-Ionizing Radiation Protection (ICNIRP) acknowledges uncertainties regarding how electrostimulation affects human neurophysiology in the ELF-MF frequency range [ICNIRP, 2020]. This

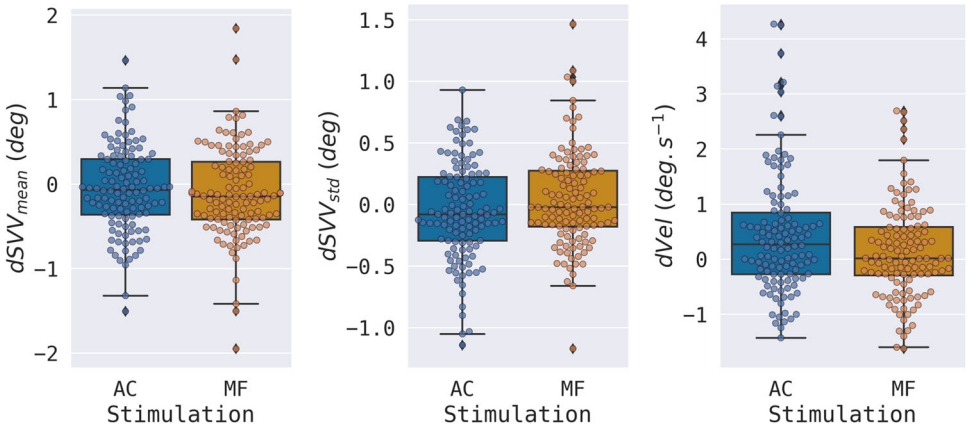

Fig. 4. Boxplot representation of dSVVmean (left panel), dSVVstd (middle panel), and dVel (right panel) distributions comparing AC and MF stimulations. Individual measurements are presented as swarm plot over each boxplot. dSVVstd ($F_{1,29} = 7.86$, $P = 0.009$, $\eta^2_G = 2\%$) and dVel ($F_{1,29} = 9.04$, $P = 0.005$, $\eta^2_G = 2\%$) yielded significant differences between AC and MF. AC = alternating current; MF = magnetic fields.

work was intended to shed light on some knowledge gap, by investigating other graded potential cells located in the vestibular system.

Considering previous work from our group [Bouisset et al., 2002a,b], we argued that ELF-MF stimulations applied laterally would more specifically trigger the vestibular hair cells within the utricular subsystem. Hence, the first aim here was to study the potential acute effect of vestibular exposure to a power-frequency MF by investigating the SVV in which the utricle plays a significant role [Jaeger et al., 2008]. Furthermore, given potential differences between AC and MF, the second aim of this work was to compare the results from both stimulations.

We hypothesized more important modulations in SVV outcomes with MF than with AC given that (i) the intensity related to AC is potentially dampened by the head's anatomical structures but not with MF and (ii) the ELF-MF stimulations would more preferentially affect the utricular system then AC. Finally, given that the utricles are best-tuned at 100 Hz and eye muscle responses progressively decrease above and under such frequency [Todd et al., 2008, 2009; Zhang et al., 2012], we also expected a frequency effect with our stimulations.

It is well known that, on average, DC impacts the SVV towards the anodal side of the stimulation [Mars et al., 2001; Volkening et al., 2014]. This was also the case in our study given that our mean SVV with DC was found at $-0.32 \pm 0.8°$. Also, given that both the SVV dotted line appearance and the anodal side were oriented towards the left, DC shortened the time to set the SVV score.

Considering previously reported results, with the intensity used in this work, our DC result was likely due to ocular torsion [Zinc et al., 1997; Watson et al., 1998b; Zink et al., 1998; Schneider et al., 2000; Severac Cauquil et al., 2003; Dalmaijer, 2018]. Thus, this validated DC as a positive control.

With AC, the current's polarity switches with frequency, and torsional eye movements should therefore be modulated accordingly. The same rational applies to our ELF-MF stimulations given their sinusoidal nature. Therefore, we didn't expect a tonic response with a stable ocular torsion generating a constant SVV error towards the same side, but rather an increased variability in the SVV results.

Even though no effect was found on dSVVmean, results show that ELF-MF performance was more variable compared to performance under AC, and it took more time for the participants to achieve verticality adjustments with the former than with the latter. This means that to get equivalent results, the adjustment performance was less optimal with ELF-MF than with AC.

Depending on the frequency, the information coming from both vestibular subsystems does not seem to be equally integrated within the vestibular nuclei. Indeed, Carriot et al. [2015] showed that as stimulation frequencies increases, more otolithic inputs than canalithic inputs are integrated. Given that our frequency range started at 20 Hz, which is often considered as the upper physiological frequency limit for the vestibular system [Cullen, 2019], the otolithic information was likely more integrated than canalithic.

Theoretically, ELF-MF [Pall, 2013] and AC [Gensberger et al., 2016] sensory-mediated responses are reported to be more specifically produced through L-type voltage-gated calcium channel (L-VGCC)

modulation. Compellingly as for the retina [Attwell, 2003], L-VGCCs are also found at the vestibular hair cell level [Juusola et al., 1996b; Rodríguez-Contreras and Yamoah, 2003; Eatock and Songer, 2011]. Therefore, as for the retina, the vestibular hair cells represent an ideal target for electrostimulation resulting from both electromagnetic induction and electric stimulations. Thus, given that equivalent L-VGCC modulation affecting the processing of information from graded potential cells could be the core explanatory mechanism for both AC and ELF-MF stimulation, we need to reflect on whether the E-Field intensity was indeed higher in ELF-MF than with AC at the utricular hair cell level.

The electrical AC stimulations applied in this study used a classical binaural bipolar montage. Thomas et al. [2020] showed that such a montage with a 1 mA stimulation intensity generates a maximum of 0.08 V/m at the vestibular system. However, such maximum E-Field value is generated at the canalithic level, whereas due to the more resistive otolithic structures, less signal is spawned at the otolithic subsystem [Thomas et al., 2020]. Based on Thomas et al.'s [2020] results, our 2 mA AC stimulations would have produced a maximum of 0.04 V/m peak at the otoliths.

The ELF-MF stimulations used here were scaled to target a constant 12.3 $T.s^{-1}_{rms}$. *dB/dt* value (Fig. 5). As in previous work from our group [Bouisset et al., 2020a,b], the in situ E-Fields at the vestibular level were estimated using the equation described in the methods. Considering a radius of 6 mm encompassing the entire vestibular system [Chacko et al., 2018], the utricular E-Fields values can be estimated at 0.053 V/m peak [Bouisset et al., 2020a].

Since E-Field values as low as 0.008 V/m are reported to be sufficient to start triggering ocular torsions [Severac Cauquil et al., 2003], it confirms that both our AC and MF stimulations were sufficiently strong to trigger vestibular-related rotational eye responses. Interestingly, the estimated E-Field level for ELF-MF was a little higher than the AC values at the utricle level (0.053 V/m peak vs. 0.04 V/m peak) and could serve as a reason for the discrepancies found in our results.

However, only the E-Fields colinear to the neuronal cell body have a maximum neurophysiological impact [Radman et al., 2009]. Therefore, depending on the orientation of the E-Fields relative to the hair cells, only a fraction of the absolute induced E-Field values could have modulated them. Thus, the maximum peak values cannot by themselves

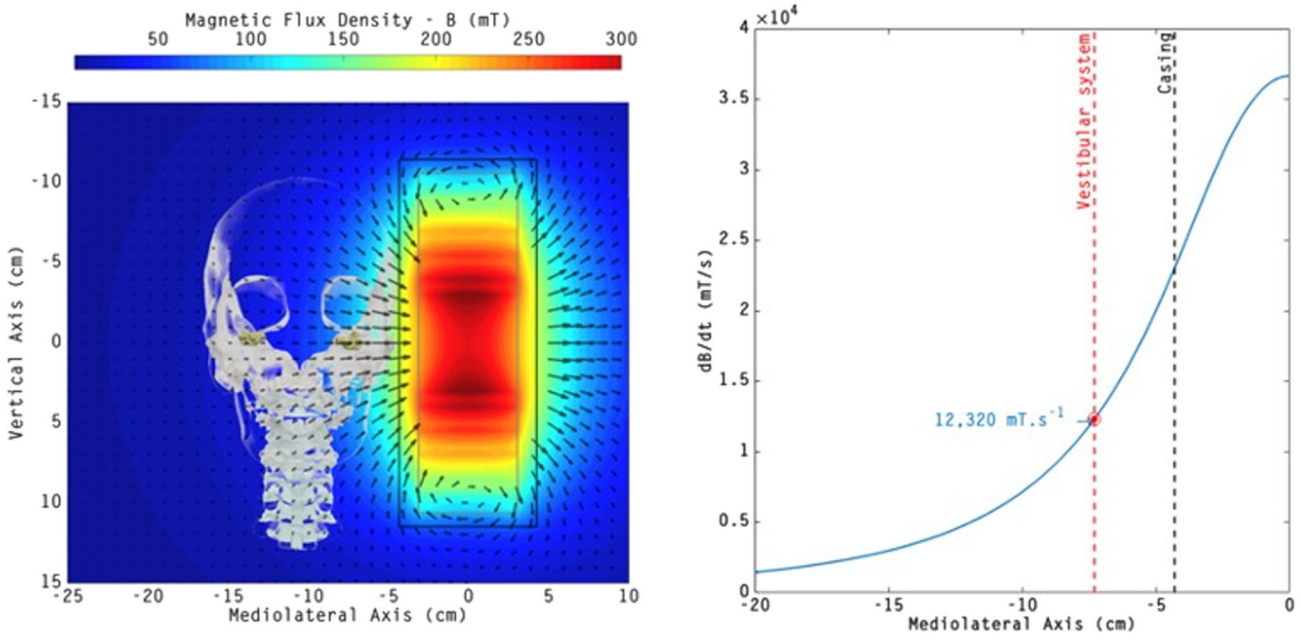

Fig. 5. Magnetic flux density distribution around the exposure device for a 20-Hz stimulation. On the left panel, the black lines show the outer boundaries casing, and the grey lines show the outer boundaries of the solenoid. The vestibular system (represented as the two yellow structures into the skull) lies approximately 3 cm from the casing of the coil. The right panel shows the *dB/dt* values along the Mediolateral axis at the vestibular level. The dashed line represents the position of the coil casing (black) and the vestibular system (red) along the mediolateral axis.

explain our results and we need information relative to the E-Fields' orientation for both stimulation modalities.

Electric stimulation modalities are applied to the skin at the skull level [Utz et al., 2010]. Given volume conduction as well as the anisotropic and non-homogeneous properties of the head's anatomical structures [Nunez and Srinivasan, 2006], the currents diffuse following the path of least resistance [Laakso and Hirata, 2013]. Depending on how the local electric vector fields align with the utricular hair cells, the relevant E-Field strength could have been much lower than the 0.04 V/m peak reported above. On the contrary, the ELF-MF goes through the anatomical structures without any hindrance, and the induced E-Fields are always orthogonal to the magnetic fields, constraining the currents in specific directions. In that regard, we have previously argued that lateral MF stimulations relative to the vestibular system induce E-Fields aligned with the utricular hair cells [Bouisset et al., 2020a]. Therefore, with MF, the utricle could have received all or close to 0.053 V/m peak E-Fields' strength.

Furthermore, the vestibular montages used between the two stimulation modalities (AC and MF) differed and should also be considered. A binaural bipolar montage was used with AC. This implies that the vestibular systems on both sides of the head are modulated in antiphase, meaning that while one system is excited, the other is inhibited. This induces a greater firing rate difference between the two systems that the brain interprets as a greater acceleration of the head in one direction. On the contrary, a left monaural lateral stimulation was used with the ELF-MF stimulations. Therefore, in this case, the firing rate in the right ear remained constant throughout the trials. For a given stimulation intensity, the binaural montages usually induce larger vestibular outcomes. Hence, the SVV results being more variable with ELF-MF would mean that the monaural lateral MF stimulation, in this case, induced a greater difference between the two vestibular systems than the binaural bipolar montage used with AC. This could only be the case if the E-Field strength at the utricular level was much higher with ELF-MF than with AC since higher stimulation intensity inflates vestibular outcome modulations [Aw et al., 2006].

Therefore, stronger and more utricular-specific ELF-MF stimulations could explain the dSVVstd difference with the AC stimulation modalities. However, caution is still needed. Indeed, if ELF-MF more specifically targeted the utricles with higher E-Field levels, greater effect size would have been expected, which is only in the order of 2% of the total variance here. Furthermore, since the utricular-specific Ovemp responses are frequency-dependent [Todd et al., 2008, 2009; Zhang et al., 2012], an effect resulting from a more important utricular modulation with ELF-MF should also lead to a frequency impact, which was not seen.

According to Dalmaijer [2018], with E-Field levels tested in the current study, modulation of SVV perception should mostly result from eye torsion. However, torsional eye movement amplitudes decrease as stimulation frequencies increase (less than 0.2° at 20 Hz) [Mackenzie and Reynolds, 2018]. Therefore, a 20-Hz stimulation may result in too small ocular torsions to be able to fully modulate SVV. Moreover, it is also suggested that with E-Fields, torsional eye movements are mostly related to canalithic activity [Reynolds and Osler, 2012; Mackenzie and Reynolds, 2018; Thomas et al., 2020], and higher frequencies such as 20 Hz are known to promote otolithic instead of canalithic activation [Carriot et al., 2015]. All these aspects are justifying the possible contribution of alternative explanations supporting our results.

The heat generated by the coil was dissipated by water cooling (the coil was made of hollow copper wire allowing cooled water circulation), which prevented heat production. Nonetheless, assuming that increased heat could have been produced, the vestibular apparatus could have been stimulated through the so-called caloric phenomenon [Shepard and Jacobson, 2016]. However, the caloric test is very well known to trigger only the horizontal canal [Shepard and Jacobson, 2016]. Thus, such phenomenon is very unlikely to alter SVV perception given that (i) the SVV outcomes are more related to otolithic activity [Jaeger et al., 2008; Kumagami et al., 2009] and (ii) the classical caloric test does not modulate SVV perception in healthy participants [Funabashi et al., 2015]. Therefore, we are confident that our results cannot be linked to any potential caloric effect.

We also made sure to minimize coil vibrations and sound production during the exposures as both are known to trigger otolithic function [Curthoys et al., 2018]. For sound to induce an otolithic response, the levels needed are usually found about 70 dB above the auditory brainstem response threshold [Curthoys et al., 2018]. Using two distinct sound level meters (RadioShack, Model 33-2055, Lake City, FL and the Sound meter android app, version 3.6.9), we made measurements of the sound level experienced by the volunteers (average of eight successive measurements = 62 dB) which is below the 70 dB level needed for the above-mentioned effect. In addition, the participants wore earplugs throughout the

entire experiment, ensuring that no confounding effect occurred. Since participants' heads were constrained against the coil, vibrations induced by the ELF-MF coil device may have triggered the vestibular hair cell, which potentially explains the difference between the two stimulation modalities. However, this is again unlikely as otolithic responses are frequency-specific [Todd et al., 2008, 2009; Zhang et al., 2012]. Indeed, the vestibular afferents are phase-locked with stimulations using frequencies much higher than 1000 Hz [Curthoys et al., 2018]. However, since no main frequency effect was found in our study, no vibration effects are expressed here.

Also, given both types of stimulations, phosphenes' perception could be acknowledged as a possible confounding factor. However, we reckon it is somewhat unlikely. First, the participants were totally naïve concerning phosphene perception and they were not trained to recognize them. In addition, it is very unlikely that participants consciously perceived or paid attention to phosphenes since their attention was fully focused on the SVV line. Second, phosphene perception threshold varies according to frequency [Lövsund et al., 1980b; Lövsund et al., 1980a; Evans et al., 2019]. In our study, phosphene perception would have been greater at 20 Hz but was certainly nonexistent at both 120 and 160 Hz [Evans et al., 2019]. Therefore, if phosphenes had been a confounding factor, we would have expected a main frequency effect. Yet, this was not the case in our study. Therefore, altogether, our results cannot be explained either by sound, vibration, or by visual perceptions, even at subconscious or subliminal levels.

The modulation of cortical regions activated by the ELF-MF signal cannot be excluded. Indeed, the position of the coil system is compatible with a potential direct effect on the temporoparietal cortices (Fig. 1). According to the model we made of our MF stimulation at 20 Hz (Fig. 5), at these cortical regions, the dB/dt levels are estimated at 20 $T.s^{-1}_{rms}$ or higher (Fig. 5, right panel), which could have modulated brain activation [Legros et al., 2015].

Interestingly, these cortical areas are implicated in spatial cognition, including the perception of spatial orientation [Hitier et al., 2014]. Otero-Millan et al., [2018] found SVV perception alterations with transcranial magnetic stimulations, showing SVV bias shift uncorrelated with torsional eye movements. Moreover, patients with temporoparietal lesions also present SVV biases [Brandt et al., 1994]. Therefore, the ELF-MF stimulations could have impacted the higher levels of multisensory processing of vestibular, somatosensory, and visual information within those brain areas [Angelaki and Cullen, 2008; Cullen, 2019], leading to modulations of SVV outcomes.

Furthermore, temporoparietal brain areas are also involved in subjective mental time perception [Arzy et al., 2009], especially during tasks implicating the vestibular system [Kaski et al., 2016].

These specific cortical regions also form the core of a complex sensory-motor network involved in motor control. Indeed, these temporoparietal brain areas interact with the motor and premotor cortices [Lopez and Blanke, 2011]. Moreover, such networks help with time and rhythm perception processing [Todd and Lee, 2015]. Therefore, the motor timing could have been impacted by the stimulation here. This is consistent with the longer SVV adjustment time we found with MF than with AC. The fact that the MF-induced E-Fields were not aligned with the cortical neuronal structures limits the potential impact on the temporoparietal cortices, which may explain the small effect sizes accounting only for 2% of the total variance for both dSVVstd and dVel.

In summary, although the differences were small, the SVV performance was less optimal with MF than with AC. This result could be due to a greater utricular activation with ELF-MF than with AC. However, given the lack of frequency effect expected for such stimulations, the position of our MF stimulation coil, and considering the *dB/dt* values generated at these sites, we cannot exclude temporoparietal cortices modulations with ELF-MF.

Further ELF-MF investigations should focus on vestibular biomarkers more specifically sensitive to E-Fields, like otolithic-specific assessments such as ocular [Cheng et al., 2009; Rosengren et al., 2009; Rosengren et al., 2010] and cervical [Watson and Colebatch, 1998; Watson et al., 1998a; Murofushi et al., 2003] vestibular evoked myogenic potentials. Lower stimulation frequencies should also be considered and the implementation of new eye-tracking techniques [Otero-Millan et al., 2015; Mackenzie and Reynolds, 2018] could help confirm and offer a better understanding of the possible eye impact reported here. Finally, targeting the temporoparietal cortices with ELF-MF stimulations would also help dissociate and disentangle the origins of the effects found herein.

Conclusion

Our results shed light on small differential effects between similar noninvasive AC and MF vestibular stimulations applied at the mastoid process. Variations in E-Fields' orientation in space relative to neuronal anatomical structures modulate the E-Fields' strength and thus the impact on such structures. These

bricks of new knowledge are of paramount importance to expand the scientific bases at the foundation of international guidelines and standards, to broaden the protection of workers and the public alike.

ACKNOWLEDGMENTS

The authors would like to thank L. Keenliside for the development and construction of the exposure head coils. The funders had no role in study design, data collection and analysis, decision to publish, study approvals, or preparation of the manuscript. This work was supported in part by Hydro-Québec, Canada, in part by Electricité De France (EDF), France, in part by Réseau de Transport d'Electricité (RTE), France, in part by the Electric Power Research Institute (EPRI), USA, in part by Mathematics of Information Technology and Complex Systems (MITACS) through the MITACS-Accelerate Program (IT05053), and in part by the National Grid and Energy Network Association (ENA), U.K.

REFERENCES

Akin FW, Murnane O. 2009. Subjective visual vertical test. Semin Hear 30:281–286.

Angelaki DE, Cullen KE. 2008. Vestibular system: The many facets of a multimodal sense. Annu Rev Neurosci 31:125–150.

Antal A, Alekseichuk I, Bikson M, Brockmöller J, Brunoni AR, Chen R, Cohen LG, Dowthwaite G, Ellrich J, Flöel A, Fregni F, George MS, Hamilton R, Haueisen J, Herrmann CS, Hummel FC, Lefaucheur JP, Liebetanz D, Loo CK, McCaig CD, Miniussi C, Miranda PC, Moliadze V, Nitsche MA, Nowak R, Padberg F, Pascual-Leone A, Poppendieck W, Priori A, Rossi S, Rossini PM, Rothwell J, Rueger MA, Ruffini G, Schellhorn K, Siebner HR, Ugawa Y, Wexler A, Ziemann U, Hallett M, Paulus W. 2017. Low intensity transcranial electric stimulation: Safety, ethical, legal regulatory and application guidelines. Clin Neurophysiol 128:1774–1809.

Arzy S, Collette S, Ionta S, Fornari E, Blanke O. 2009. Subjective mental time: The functional architecture of projecting the self to past and future. Eur J Neurosci 30:2009–2017.

Attwell D. 2003. Interaction of low frequency electric fields with the nervous system: The retina as a model system. Radiat Prot Dosimetry 106:341–348.

Aw ST, Todd MJ, Halmagyi GM. 2006. Latency and initiation of the human vestibuloocular reflex to pulsed galvanic stimulation. J Neurophysiol 96:925–930.

Bakeman R. 2005. Recommended effect size statistics for repeated measures designs. Behav Res Methods 37:379–384.

Böhmer A, Rickenmann J. 1995. The subjective visual vertical as a clinical parameter of vestibular function in peripheral vestibular diseases. J Vestib Res 5:35–45.

Bouisset N, Villard S, Legros A. 2020a. Human postural responses to high vestibular specific extremely low-frequency magnetic stimulations. IEEE Access 8:165387–165395.

Bouisset N, Villard S, Legros A. 2020b. Human postural control under high levels of extremely low frequency magnetic fields. IEEE Access 8:101377–101385.

Brandt T, Dieterich M, Danek A. 1994. Vestibular cortex lesions affect the perception of verticality. Ann Neurol 35:403–412.

Bresciani J-P, Blouin J, Popov K, Sarlegna F, Bourdin C, Vercher J-L, Gauthier GM. 2002. Vestibular signals contribute to the online control of goal-directed arm movements. Curr Psycholgy Cogn 21:263–280.

Carriot J, Jamali M, Chacron MJ, Cullen KE. 2014. Statistics of the vestibular input experienced during natural self-motion: Implications for neural processing. J Neurosci 34: 8347–8357.

Carriot J, Jamali M, Brooks JX, Cullen KE. 2015. Integration of canal and otolith inputs by central vestibular neurons is subadditive for both active and passive self-motion: Implication for perception. J Neurosci 35:3555–3565.

Chacko LJ, Schmidbauer DT, Handschuh S, Reka A, Fritscher KD, Raudaschl P, Saba R, Handler M, Schier PP, Baumgarten D, Fischer N, Pechriggl EJ, Brenner E, Hoermann R, Glueckert R, Schrott-fischer A. 2018. Analysis of vestibular labyrinthine geometry and variation in the human temporal bone. Front Neurosci 12:1–13.

Cheng PW, Chen CC, Wang SJ, Young YH. 2009. Acoustic, mechanical and galvanic stimulation modes elicit ocular vestibular-evoked myogenic potentials. Clin Neurophysiol 120:1841–1844.

Cullen KE. 2019. Vestibular processing during natural self-motion: Implications for perception and action. Nat Rev Neurosci 20:346–363.

Curthoys IS. 2010. A critical review of the neurophysiological evidence underlying clinical vestibular testing using sound, vibration and galvanic stimuli. Clin Neurophysiol 121:132–144.

Curthoys IS. 2017. The new vestibular stimuli: Sound and vibration—Anatomical, physiological and clinical evidence. Exp Brain Res 235:957–972.

Curthoys IS, Grant JW, Burgess AM, Pastras CJ, Brown DJ, Manzari L. 2018. Otolithic receptor mechanisms for vestibular-evoked myogenic potentials: A review. Front Neurol 9:1–15.

Dakin CJ, Son GML, Inglis JT, Blouin J-S. 2007. Frequency response of human vestibular reflexes characterized by stochastic stimuli. J Physiol 583:1117–1127.

Dalmaijer E. 2018. Beyond the vestibulo-ocular reflex: Vestibular input is processed centrally to achieve visual stability. Vision 2:1–21.

Day BL, Ramsay E, Welgampola MS, Fitzpatrick RC. 2011. The human semicircular canal model of galvanic vestibular stimulation. Exp Brain Res 210:561–568.

Dieterich M, Brandt T. 1993. Ocular torsion and tilt of subjective visual vertical are sensitive brainstem signs. Ann Neurol 33:292–299.

Dieterich M, Brandt T. 2019. Perception of verticality and vestibular disorders of balance and falls. Front Neurol 10:1–15.

Dlugaiczyk J, Gensberger KD, Straka H. 2019. Galvanic vestibular stimulation: From basic concepts to clinical applications. J Neurophysiol 121:2237–2255.

Eatock RA, Songer JE. 2011. Vestibular hair cells and afferents: Two channels for head motion signals. Annu Rev Neurosci 34:501–534.

Evans ID, Palmisano S, Loughran SP, Legros A, Croft RJ. 2019. Frequency-dependent and montage-based differences in phosphene perception thresholds via transcranial alternating current stimulation. Bioelectromagnetics 40:365–374.

Fitzpatrick R, Burke D, Gandevia SC. 1996. Loop gain of reflexes controlling human standing measured with the use of postural and vestibular disturbances. J Neurophysiol 76:3994–4008.

Fitzpatrick RC, Day BL. 2004. Probing the human vestibular system with galvanic stimulation. J Appl Physiol 96:2301–2316.

Forbes PA, Dakin CJ, Vardy AN, Happee R, Siegmund GP, Schouten AC, Blouin J-S. 2013. Frequency response of vestibular reflexes in neck, back, and lower limb muscles. J Neurophysiol 110:1869–1881.

Friedmann G. 1970. The judgement of the visual vertical and horizontal with peripheral and central vestibular lesions. Brain 93:313–328.

Funabashi M, Flores AI, Vicentino A, Barros CGC, Pontes-Neto OM, Leite JP, Santos-Pontelli TEG. 2015. Subjective visual vertical during caloric stimulation in healthy subjects: Implications to research and neurorehabilitation. Rehabil Res Pract 2015:1–4.

Gensberger KD, Kaufmann A-K, Dietrich H, Branoner F, Banchi R, Chagnaud BP, Straka H. 2016. Galvanic vestibular stimulation: Cellular substrates and response patterns of neurons in the vestibulo-ocular network. J Neurosci 36:9097–9110.

Hitier M, Besnard S, Smith PF. 2014. Vestibular pathways involved in cognition. Front Integr Neurosci 8:1–16.

ICNIRP. 2010. Guidelines for limiting exposure to time-varying electric and magnetic fields (1 Hz to 100 kHz). Health Phys 99:818–836.

ICNIRP. 2020. Gaps in knowledge relevant to the "Guidelines for Limiting Exposure to Time-Varying Electric and Magnetic Fields (1 Hz-100 kHz)." Health Phys 118:533–542.

IEEE. 2002. C95.6. IEEE Standard for Safety Levels with Respect to Human Exposure to Electromagnetic Fields, 0-3kHz. IEEE New York. New York: The Institute of Electrical and Electronics Engineers.

IEEE. 2019. IEEE Standard for Safety Levels With Respect to Human Exposure to Electric, Magnetic, and Electromagnetic Fields, 0 Hz to 300 GHz. IEEE Std C95.1-2005 (Revision IEEE Std C95.1-1991). Vol 2005.

Jaeger R, Kondrachuk AV, Haslwanter T. 2008. The distribution of otolith polarization vectors in mammals: Comparison between model predictions and single cell recordings. Hear Res 239:12–19.

Johnson P, Besselsen D. 2002. Practical aspects of experimental design in animal research experimental design: Initial steps. Inst Lab Anim Res 43:203–206.

Juusola M, French AS, Uusitalo RO, Weckström M. 1996a. Information processing by graded-potential transmission through tonically active synapses. Trends Neurosci 19:292–297.

Juusola M, French AS, Uusitalo RO, Weckström M. 1996b. Information processing by graded-potential transmission through tonically active synapses. Trends Neurosci 19:292–297.

Kaski D, Quadir S, Nigmatullina Y, Malhotra PA, Bronstein AM, Seemungal BM. 2016. Temporoparietal encoding of space and time during vestibular-guided orientation. Brain 139:392–403.

Kumagami H, Sainoo Y, Fujiyama D, Baba A, Oku R, Takasaki K, Shigeno K, Takahashi H. 2009. Subjective visual vertical in acute attacks of Ménière's disease. Otol Neurotol 30:206–209.

Kwan A, Forbes PA, Mitchell DE, Blouin J-S, Cullen KE. 2019. Neural substrates, dynamics and thresholds of galvanic vestibular stimulation in the behaving primate. Nat Commun 10:1–15.

Laakso I, Hirata A. 2013. Computational analysis shows why transcranial alternating current stimulation induces retinal phosphenes. J Neural Eng 10:1–9.

Laakso I, Kännälä S, Jokela K. 2013. Computational dosimetry of induced electric fields during realistic movements in the vicinity of a 3 T MRI scanner. Phys Med Biol 58:2625–2640.

Legros A, Modolo J, Brown S, Roberston J, Thomas AW. 2015. Effects of a 60 Hz magnetic field exposure up to 3000 μT on human brain activation as measured by functional magnetic resonance imaging. PLoS One 10:1–27.

Lopez C, Blanke O. 2011. The thalamocortical vestibular system in animals and humans. Brain Res Rev 67:119–146. https://doi.org/10.1016/j.brainresrev.2010.12.002

Lövsund P, Öberg PÅ, Nilsson SEG, Reuter T. 1980a. Magnetophosphenes: A quantitative analysis of thresholds. Med Biol Eng Comput 18:326–334.

Lövsund P, Öberg P, Nilsson SEG. 1979. Quantitative determination of thresholds of magnetophosphenes. Radio Sci 14:199–200.

Lövsund P, Oberg PA, Nilsson SEG. 1980b. Magneto- and electrophosphenes: A comparative study. Med Biol Eng Comput 18:758–764.

Mackenzie SW, Reynolds RF. 2018. Ocular torsion responses to sinusoidal electrical vestibular stimulation. J Neurosci Methods 294:116–121.

Mars F, Popov K, Vercher JL. 2001. Supramodal effects of galvanic vestibular stimulation on the subjective vertical. Neuroreport 12:2991–2994.

Mars F, Vercher JL, Popov K. 2005. Dissociation between subjective vertical and subjective body orientation elicited by galvanic vestibular stimulation. Brain Res Bull 65:77–86.

Min KK, Ha JS, Kim MJ, Cho CH, Cha HE, Lee JH. 2007. Clinical use of subjective visual horizontal and vertical in patients of unilateral vestibular neuritis. Otol Neurotol 28:520–525.

Murofushi T, Monobe H, Ochiai A, Ozeki HTM, HMAO. 2003. The site of lesion in "vestibular neuritis": Study by galvanic VEMP. Neurology 61:417–418.

Van Nierop LE, Slottje P, Kingma H, Kromhout H. 2013. MRI-related static magnetic stray fields and postural body sway: A double-blind randomized crossover study. Magn Reson Med 70:232–240.

Norris CH, Miller AJ, Perin P, Holt JC, Guth PS. 1998. Mechanisms and effects of transepithelial polarization in the isolated semicircular canal. Hear Res 123:31–40.

Nunez PL, Srinivasan R. 2006. Electric Fields of the Brain: The Neurophysics of EEG. New York, NY: Oxford University Press. pp. 26–31.

Oman C. 2007. Spatial Processing in Navigation, Imagery and Perception. New York, NY: Springer. pp. 209–247.

Otero-Millan J, Roberts DC, Lasker A, Zee DS, Kheradmand A. 2015. Knowing what the brain is seeing in three dimen-

sions: A novel, noninvasive, sensitive, accurate, and low-noise technique for measuring ocular torsion. J Vis 15:1–15.

Otero-Millan J, Winnick A, Kheradmand A. 2018. Exploring the role of temporoparietal cortex in upright perception and the link with torsional eye position. Front Neurol 9:1–10.

Pagarkar W, Bamiou D-E, Ridout D, Luxon LM. 2013. Subjective visual vertical and horizontal. Arch Otolaryngol Neck Surg 134:394–401.

Pall ML. 2013. Electromagnetic fields act via activation of voltage-gated calcium channels to produce beneficial or adverse effects. J Cell Mol Med 17:958–965.

Pavlik AE, Inglis JT, Lauk M, Oddsson L, Collins JJ. 1999. The effects of stochastic galvanic vestibular stimulation on human postural sway. Exp Brain Res 124:273–280.

Radman T, Ramos RL, Brumberg JC, Bikson M. 2009. Role of cortical cell type and morphology in subthreshold and suprathreshold uniform electric field stimulation in vitro. Brain Stimul 2:215–228.

Reynolds RF, Osler CJ. 2012. Galvanic vestibular stimulation produces sensations of rotation consistent with activation of semicircular canal afferents. Front Neurol 3:1–2.

Rodríguez-Contreras A, Yamoah EN. 2003. Effects of permeant ion concentrations on the gating of L-type Ca2+ channels in hair cells. Biophys J 84:3457–3469.

Rosengren SM, Welgampola MS, Colebatch JG. 2010. Vestibular evoked myogenic potentials: Past, present and future. Clin Neurophysiol 121:636–651.

Rosengren SM, Jombik P, Halmagyi GM, Colebatch JG. 2009. Galvanic ocular vestibular evoked myogenic potentials provide new insight into vestibulo-ocular reflexes and unilateral vestibular loss. Clin Neurophysiol 120:569–580.

Schaap K, Portengen L, Kromhout H. 2015. Exposure to MRI-related magnetic fields and vertigo in MRI workers. Occup Environ Med 73:161–166.

Schneider E, Glasauer CAS, Dieterich M. 2000. Central processing of human ocular torsion analyzed by galvanic vestibular stimulation. Neuroreport 11:1559–1563.

Severac Cauquil A, Faldon M, Popov K, Day BL, Bronstein AM. 2003. Short-latency eye movements evoked by near-threshold galvanic vestibular stimulation. Exp Brain Res 148:414–418.

Shepard NT, Jacobson GP. 2016. The caloric irrigation test. Handb Clin Neurol 137:119–131.

Srinivasan R, Tucker DM, Murias M. 1998. Estimating the spatial Nyquist of the human EEG. Behav Res Methods Instruments Comput 30:8–19.

Stephan T, Deutschländer A, Nolte A, Schneider E, Wiesmann M, Brandt T, Dieterich M. 2005. Functional MRI of galvanic vestibular stimulation with alternating currents at different frequencies. Neuroimage 26:721–732.

Thomas C, Truong D, Clark TK, Datta A. 2020. Understanding current flow in Galvanic Vestibular Stimulation: A Computational Study. 2020 42nd Annu Int Conf IEEE Eng Med Biol Soc Montreal, QC. Canada: IEEE. pp. 2442–2446.

Todd NPM, Lee CS. 2015. The sensory-motor theory of rhythm and beat induction 20 years on: A new synthesis and future perspectives. Front Hum Neurosci 9:1–25.

Todd NPM, Rosengren SM, Colebatch JG. 2009. A utricular origin of frequency tuning to low-frequency vibration in the human vestibular system? Neurosci Lett 451:175–180.

Todd NPM, Rosengren SM, Colebatch JG. 2008. Tuning and sensitivity of the human vestibular system to low-frequency vibration. Neurosci Lett 444:36–41.

Utz KS, Dimova V, Oppenländer K, Kerkhoff G. 2010. Electrified minds: Transcranial direct current stimulation (tDCS) and galvanic vestibular stimulation (GVS) as methods of non-invasive brain stimulation in neuropsychology—A review of current data and future implications. Neuropsychologia 48:2789–2810.

Vibert D, Häusler R, Safran AB. 1999. Subjective visual vertical in peripheral unilateral vestibular diseases. J Vestib Res Equilib Orientat 9:145–152.

Volkening K, Bergmann J, Keller I, Wuehr M, Müller F, Jahn K. 2014. Verticality perception during and after galvanic vestibular stimulation. Neurosci Lett 581:75–79.

Watson SRD, Fagan P, Colebatch JG. 1998a. Galvanic stimulation evokes short-latency EMG responses in sternocleidomastoid which are abolished by selective vestibular nerve section. Electroencephalogr Clin Neurophysiol—Electromyogr Mot Control 109:471–474.

Watson SRD, Brizuela AE, Curthoys IS, Colebatch JG, MacDougall HG, Halmagyi GM. 1998b. Maintained ocular torsion produced by bilateral and unilateral galvanic (DC) vestibular stimulation in humans. Exp Brain Res 122:453–458.

Watson S, Colebatch J. 1998. Vestibulocollic reflexes evoked by short-duration galvanic stimulation in man. J Physiol 513:587–597.

Yu JF, Lee KC, Wang RH, Chen YS, Fan CC, Peng YC, Tu TH, Chen CI, Lin KY. 2015. Anthropometry of external auditory canal by non-contactable measurement. Appl Ergon 50:50–55.

Zenner HP, Reuter G, Hong S, Zimmermann U, Gitter AH. 1992. Electrically evoked motile responses of mammalian type I vestibular hair cells. J Vestib Res 2:181–191.

Zhang AS, Govender S, Colebatch JG. 2012. Tuning of the ocular vestibular evoked myogenic potential to bone-conducted sound stimulation. J Appl Physiol 112:1279–1290.

Zinc R, Steddin S, Weiss A, Brandt T, Dieterich M. 1997. Galvanic vestibular stimulation in humans: effects on otolith function in roll. Neurosci Lett 232:171–174.

Zink R, Bucher SF, Weiss A, Brandt T, Dieterich M. 1998. Effects of galvanic vestibular stimulation on otolithic and semicircular canal eye movements and perceived vertical. Electroencephalogr Clin Neurophysiol 107:200–205.